

# **STUDY REPORT**

**SR313 (2015)**

## **WEATHERTIGHTNESS OF FLASHINGS AND THE IMPORTANCE OF UPSTAND HEIGHTS**

**Mark Bassett and  
Greg Overton**



**MINISTRY OF BUSINESS,  
INNOVATION & EMPLOYMENT**  
HĪKINA WHAKATUTUKI

The work reported here was jointly funded by BRANZ from the Building Research Levy and the Ministry of Business, Innovation and Employment.

© BRANZ 2015  
ISSN: 1179-6197

## **Preface**

This is the first of a series of reports prepared during research into the weathertightness of junctions between building materials and systems.

## **Acknowledgements**

This work was funded by the Ministry of Business, Innovation and Employment and the Building Research Levy. The assistance of Roger Stanford is gratefully acknowledged.

## **Note**

This report is primarily intended for building science researchers, but it also contains material that will be of value to cladding manufacturers.

# **WEATHERTIGHTNESS OF FLASHINGS AND THE IMPORTANCE OF UPSTAND HEIGHTS**

**BRANZ Study Report SR313 (2015)**

**Mark Bassett and Greg Overton**

## **Abstract**

This paper examines the weathertight performance of three common junctions in wall claddings and the approach taken to flashing these joints in New Zealand residential buildings. It makes a start towards understanding the leakage performance of joints and how they might be modified to extend their range of application to taller buildings. The joints investigated are:

- horizontal H and Z jointers between direct-fixed sheet claddings
- the window head flashing in a cavity wall
- a horizontal apron flashing at the junction between a roof and wall.

A general trend was observed for joints to resist water leakage to pressures equivalent to the upstand height head of water as long as there were no air leakage paths through the joint. Adding vents for cavity walls or gaps due to construction tolerances allowed air-carried water past the upstand at lower pressures. However, this was always well above the 50 Pa 'wetwall test' pressure adopted in E2/VM1 for claddings on a cavity wall. For H and Z jointers, the leakage onset pressure was 100–300 Pa when the gap between flashing and cladding exceeded 2–3 mm. With an air leakage path in the joint, both upstand height and the presence of a hem did little to resist water entry.

Water leakage over a window head flashing occurred at slightly lower pressures (100–150 Pa) as a consequence of the joint including vents. However, opportunities were found to improve the way this joint handles run-off by increasing the clearance between the cladding and flashing. The dynamic leakage characteristics were found to be frequency dependent, unlike for H and Z jointers, because of the inertia of larger volumes of water in the joint. The apron flashing was also a vented joint but it coped with run-off better than a window head joint because of the larger 35 mm vertical gap between the cladding and apron. However, the joint was found to be prone to wind-carried rain leakage, which is consistent with field observations. Further work will be needed to link this performance with wind and rain exposure on building façades.

## **Keywords**

Weathertightness, Upstands, Flashings, Junctions

<b>Contents</b>	<b>Page</b>
<b>1. INTRODUCTION.....</b>	<b>1</b>
<b>2. TEST WIND PRESSURES AND SPRAY RATES.....</b>	<b>3</b>
<b>3. MEASURED RAIN LEAKAGE CHARACTERISTICS.....</b>	<b>3</b>
<b>4. TYPICAL FLASHED JOINTS SEEN IN RESIDENTIAL BUILDINGS.....</b>	<b>5</b>
<b>5. LEAKAGE CHARACTERISTICS OF A HORIZONTAL CLADDING JOINTER.....</b>	<b>7</b>
<b>5.1 Significance of offset (air gaps) between the jointer and the cladding.....</b>	<b>7</b>
<b>5.2 Significance of a hem on the upstand of the jointer.....</b>	<b>9</b>
<b>6. LEAKAGE CHARACTERISTICS OF CAVITY CLOSER IN A WINDOW HEAD JOINT.....</b>	<b>11</b>
<b>6.1 Dependency of onset leakage pressures on run-off rate.....</b>	<b>13</b>
<b>6.2 Dependency of onset leakage pressures on gap between cladding and head         flashing.....</b>	<b>14</b>
<b>6.3 Leakage with dynamic wind pressures applied.....</b>	<b>15</b>
<b>7. LEAKAGE CHARACTERISTICS OF AN APRON FLASHING TO ROOF JOINT.....</b>	<b>17</b>
<b>7.1 Wind-driven water leakage past the apron flashing.....</b>	<b>18</b>
<b>8. CONCLUSIONS.....</b>	<b>19</b>
<b>9. ACKNOWLEDGEMENTS.....</b>	<b>20</b>
<b>10. REFERENCES.....</b>	<b>21</b>

<b>Figures</b>	<b>Page</b>
Figure 1. Location of water entry in New Zealand leaking buildings. ....	1
Figure 2. Equipment for measuring the weathertightness characteristics of joints. ....	4
Figure 3. Time dependency of leakage through the cavity closer above a window head flashing. ....	5
Figure 4. A selection of flashings used in New Zealand buildings and taken from E2/AS1. ....	6
Figure 5. Sectional view through an H jointer between two sheets of wall cladding. ....	7
Figure 6. Air pressures at which water leakage occurs through the H jointer as a function of upstand height and the offset gap width. ....	8
Figure 7. Steady pressure leakage characteristics of flashings with 35 mm and 60 mm upstands with and without hems. ....	9
Figure 8. Dynamic leakage characteristics of flashings with a 35 mm upstand and a hem. ....	10
Figure 9. A comparison of measured and calculated leakage rates with fluctuating air pressures. ....	11
Figure 10. Experimental window head joint with cavity closer and variable joint dimensions. ....	11
Figure 11. Deposition rate of water as a function of height above the cavity closer. ....	13
Figure 12. Pressure difference at the onset of leakage through a window head joint as a function of run-off rate over the joint. ....	14
Figure 13. Pressure at which water first appeared in the cavity closer as a function of run-off rate over the window head joint. ....	14
Figure 14. A pictorial view of leakage through a window head joint with varying surface run-off rates and gap dimension (g) between upper cladding and head flashing. ....	15
Figure 15. Frequency dependency of relationship between peak pressure and water leakage into a window head joint. ....	16
Figure 16. A comparison of measured and calculated leakage rates using a simplified model. ....	16
Figure 17. Experimental apron flashing joint between roof. ....	17
Figure 18. Water leakage rates through the cavity closer above an apron flashing. ....	18
Figure 19. Mass flow of water reaching various heights above the base of the cavity closer of an apron flashing. ....	19

<b>Tables</b>	<b>Page</b>
Table 1. Spray nozzle operating conditions and run-off rates over horizontal joints. ....	4
Table 2. Spray nozzle operating conditions and run-off rates over the joint. ....	18

# 1. INTRODUCTION

Most water leaks in residential buildings occur at joints between claddings and components such as windows. This was confirmed by a survey of leaking buildings in New Zealand (Bassett et al. 2003) during the leaking building crisis in the late 1990s and early 2000s. Figure 1 assigns over 60% of leakage sites to junctions between claddings and other components and less than 40% to the roof and wall claddings. Traditional metal flashings were found to have been replaced with sealants in this survey, and many of the buildings were found to offer little protection from the weather due to lack of eaves. In most cases, barrier-clad walls were not designed to manage water leaks, and this allowed water to accumulate over time, leading to decayed timber framing. A similar fraction (26%) of water entry points in Canadian buildings were identified around window and door junctions with claddings in a survey of leaking buildings in British Columbia (Morrison Hershfield Limited 1996). In this survey, 90% of water leakage sites were found to be at junctions between materials and components or at penetrations through the cladding.

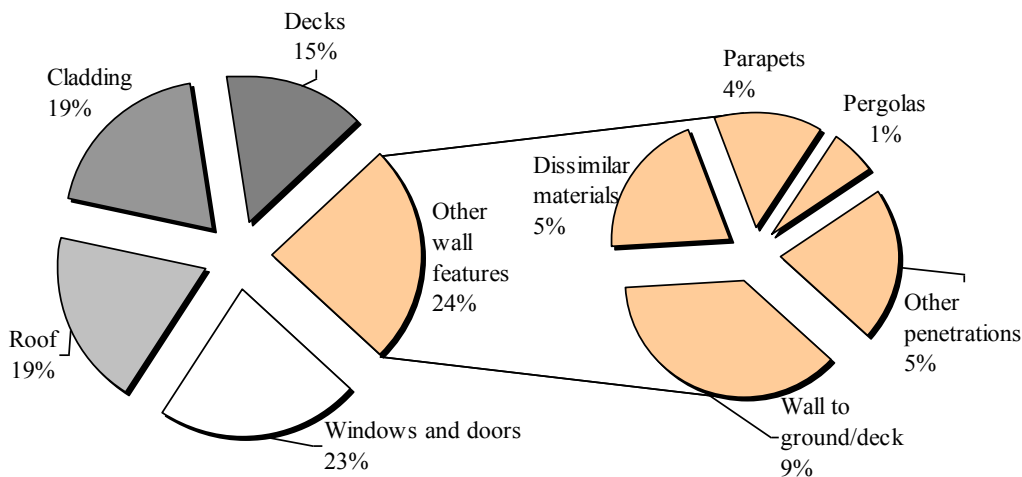


Figure 1. Location of water entry in New Zealand leaking buildings.

The then Department of Building and Housing (now the Ministry of Business, Innovation and Employment) responded to the leaking building problem by modifying the Approved Document E2/AS1 *External moisture* of the New Zealand Building Code (NZBC). The intent was to improve the standard of water management in wall and roof designs (Department of Building and Housing 2005a). Most of the changes were based on the 4Ds (deflection, drainage, drying and durability) approach developed in Canada by Hazleden and Morris (1999) and incorporated a water-managed cavity behind the cladding.

The associated NZBC Verification Method test procedure E2/VM1 (Department of Building and Housing 2005b) defined performance criteria that apply to claddings and flashings in cavity walls:

- Water should not systematically reach the dry side of the cavity during any of the tests (including above the upstand on horizontal flashings above cavity closers).
- The first test in E2/VM1 is a static and cyclic pressure test of the complete wall system.
- The second test introduces defects in the cladding around flashings to confirm that water is successfully controlled by drainage paths including the back of the cladding and flashings at junctions between components or different claddings.

- Finally, the 'wetwall test' applies 50 Pa pressure difference across the cladding and checks that water leaks through the cladding are confined to the drainage paths and do not bridge the cavity.

These tests applied the following criteria to flashings in cavity walls:

- The flashing forms part of the drainage path for water on the back of the cladding.
- The flashing must rainscreen the joint and prevent water from reaching the underlay with a rain intensity of at least 3 l/m<sup>2</sup>.min and a 50 Pa air pressure difference between the wetwall and the cavity.

For walls with direct-fixed claddings, the normal practice had been to follow AS/NZS 4284:2008 *Testing of building facades* and, for window systems, NZS 4211:2008 *Specification for performance of windows*. However, there are many questions concerning the performance of flashings that are not answered by these procedures, which this research is starting to address:

- How far should the flashing upstand extend upwards behind the cladding to deal with wind-driven rain?
- Do the upstand heights of flashings need to be adjusted to cope with rain bouncing of a roof? (This is particularly important for apron flashings between roof and wall.)
- Do cavity closers have a role in managing air and water entry through the joint?
- How should cladding to flashing clearances be sized to control run-off?
- Do hems folded into metal flashings improve the weathertightness performance in contact with direct-fixed claddings?
- How should the performance of flashings in walls with direct-fixed claddings be measured?

Perhaps the most pressing need for research on the leakage performance of joints is in support of cladding designs for buildings above the height limit for E2/AS1 (three storeys maximum but nominally 10 m above ground). This includes very tall buildings, which tend to apply an engineered and tested curtain wall. Many of these in-between buildings adapt E2/AS1 (updated in 2011) cladding and flashings to timber-framed infill panels. These are more exposed to high wind pressures and higher surface run-off rates than is the case for a low-rise residential building. A scientific approach that measures the performance characteristics of flashings and relates this to wind speeds and run-off rates is likely to help extend the applicability of E2/AS1 details. It will also show how they might usefully be adapted for taller buildings.

There are numerous illustrations of flashings in practical building literature. However, there are few scientific investigations of the water leakage performance of joints and how their design might be developed to cope with extreme exposure. One of the earliest investigations (Ishikawa 1974) measured the leakage characteristics of seven joints from a metal curtain wall. The study concluded that the key elements were a large external opening to prevent a water film from bridging the gap and an airtight internal joint to support wind pressures. These results are not applicable to joints in rainscreen walls where only limited pressure moderation can be expected across the wet surfaces.

More recent studies have measured leakage rates through specific defects in walls (Lacasse et al. 2003; Sahal and Lacasse 2004) and independently by Teasdale-St-Hilaire and Derome (2006). The earlier work of Lacasse and Sahal measured water leakage rates through defects in walls, such as missing lengths of sealant. They used the leakage function of wind pressure and rain load to estimate the moisture loads that have to be managed by vapour diffusion and

ventilation drying within the wall. Water leakage rates were measured as a function of run-off rates and static wind pressure on the wall. These were fitted to an empirical relationship that was then used to estimate moisture entry loads in a range of North American climates. A similar approach to measuring water entry functions for weatherboard claddings was followed by Bassett et al. (2012), leading to predicted water entry loads. These could then be compared with the capacity for ventilation drying inside the water-managed cavity in a variety of New Zealand city climates.

## **2. TEST WIND PRESSURES AND SPRAY RATES**

Until recently, the test pressures and rain loads in E2/VM1 were adopted from the NZS 4211:2008 and AS/NZ 4284:2008 standard tests for windows and walls respectively. This was on the basis that test pressures and spray rates have evolved over time to align with acceptable field performance. More recently, test pressures were adjusted in E2/VM1 (2011) to align with AS/NZS 1170:2002 *Structural design actions*, which provides a calculation path for ultimate limit state and serviceability limit wind pressures. The test pressures for whole-wall weathertightness tests have been indexed to 30% of the serviceability pressure for a building in an extra high wind zone. Wind pressures and rain loads on the vertical surfaces of buildings in New Zealand have been examined by Overton (2013) as part of a recent review of test pressures and spray rates in E2/VM1 (2011). This analysis showed that pressures in E2/VM1 exceed the 5-year return wind pressures (normalised for site exposure) for the majority of locations in New Zealand. The spray rate from E2/VM1 was higher than the 5-year return wind-driven rain rate for approximately half the locations. However, the majority of site wind pressures (and hence wind-driven rain rates) are likely to be lower than normalised values because most sites will be in more sheltered locations.

Similar methods to those used to calculate wind pressures and wind-driven rain rates have been used to explore the leakage performance of residential weatherboard cladding systems by Bassett et al. (2014). Climate files of rain loads and wind pressures were generated for 14 New Zealand cities and used with leakage functions for weatherboard and brick veneer claddings to estimate leakage rates. These were then compared with the capacity for ventilation drying in WALLDRY-NZ – a tool developed for educational purposes (Bassett et al. 2012). These calculations require leakage rate functions of rain load and wind pressure. They have to be derived experimentally using methods that are similar to standard weathertight test procedures but vary the rain intensity and wind pressure and measure the actual water leakage rates. This research is starting to gather leakage functions for individual joints, with a long-term plan to optimise the geometry of joints and flashings for the demands of location and exposure.

## **3. MEASURED RAIN LEAKAGE CHARACTERISTICS**

Equipment illustrated in Figure 2 was used to measure the water leakage characteristics of joints between building components. It consists of a pressure chamber linked to a fan and a fluctuating piston that together apply a steady pressure and a superimposed fluctuating pressure across the specimen. The pressure amplitude can be changed by adjusting the piston stroke, although below 0.2 Hz, there was simply not enough travel to reach large pressure amplitudes. The wall specimen measured 0.7 x 0.7 m (area 0.49 m<sup>2</sup>), and the length of joint under investigation was 0.53 m.



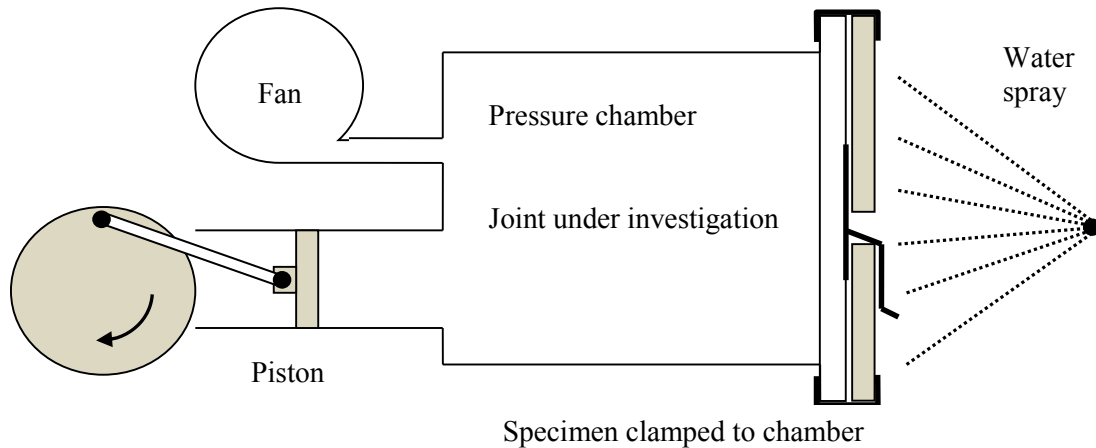


**Figure 2. Equipment for measuring the weathertightness characteristics of joints.**

A range of water spray nozzles were used to wet the sample area with between 3.4 l/m<sup>2</sup>.min (corresponding to the minimum rain load called for in E2/VM1 2005) and 0.08 l/m<sup>2</sup>.min. This is similar to the rain loads applied to large wall assemblies (0.02–3 l/m<sup>2</sup>.min) by Bassett et al. (2014). It provides a wide enough range of rain intensity to develop rain leakage functions that include most rain events. In these measurements, the run-off rate was found to be a better measure of water delivered to the joint and is recorded in Table 1 for each nozzle at normal operating conditions.

**Table 1. Spray nozzle operating conditions and run-off rates over horizontal joints.**

Nozzle description	Water pressure (bar)	Air pressure (bar)	Stand-off (m)	Run-off rate (g/m.s)
Promax QPHA-2 Gray	2.8	N/A	1.2	9.8
Promax QPHA-1.5 White	2.8	N/A	1.2	4.3
Promax QPHA-1 Brown	2.8	N/A	1.2	1.3
Unijet TPU800067	2.8	N/A	0.78	2.4
Unijet TPU650033	2.8	N/A	0.70	1.5
Unijet TPU650017	2.8	N/A	0.56	0.57
Spraying Systems PA67-6-20-70	2.8	0.6	0.52	0.56
Spraying Systems PA67-6-20-70	2.8	1.0	0.52	0.96

*Note: All of the water sprays were operated at normal mains water pressure except the Spraying Systems PA67-6-20-70 atomising nozzle, which was used to reach the lowest run-off rates.*

Water leakage rates through joints were measured gravimetrically using a strip of water-absorbing material placed just above the end of the flashing. This absorbent material was a commercial cleaning material (Wettex) composed primarily of cotton and cellulose fibres. The spraying rate and pressure condition was maintained for 1 minute throughout all measurements. This gave a few seconds to establish water flow over the joint and sufficient time in which to measure an average leakage rate. Figure 3 shows the water entry rate through the cavity closer above a window head flashing for a range of measurement periods from 1–15 minutes. The uncertainties here characterise the repeatability of measurements.

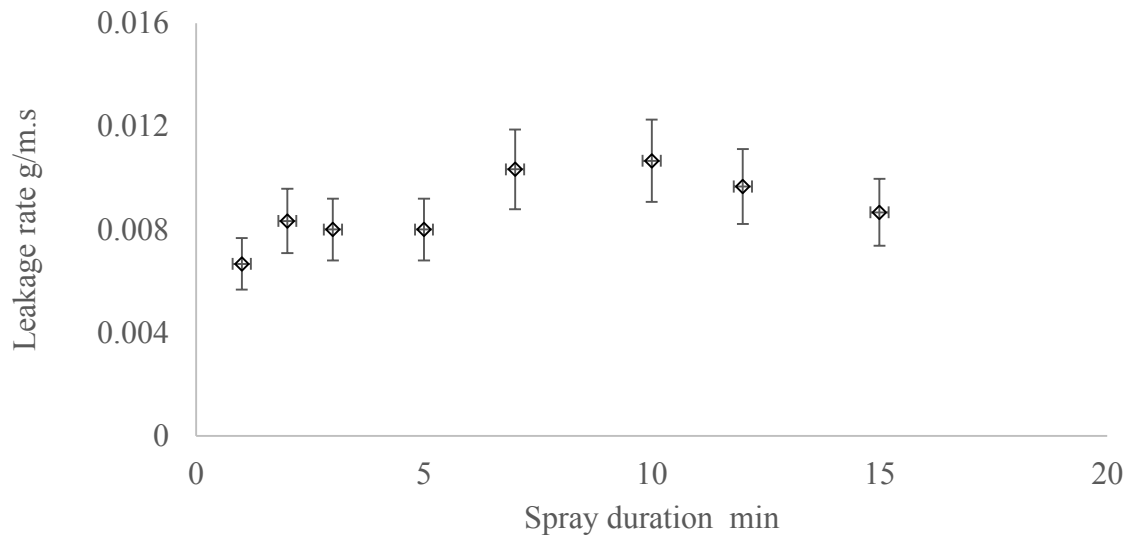


**Figure 3. Time dependency of leakage through the cavity closer above a window head flashing.**

#### **4. TYPICAL FLASHED JOINTS SEEN IN RESIDENTIAL BUILDINGS**

There are a large number of joints described in E2/AS1 (2011). However, the three junctions illustrated in Figure 4 capture most of the essential features of flashings and their application in walls with cavities or direct-fixed claddings. The three joints chosen for what is a preliminary study are:

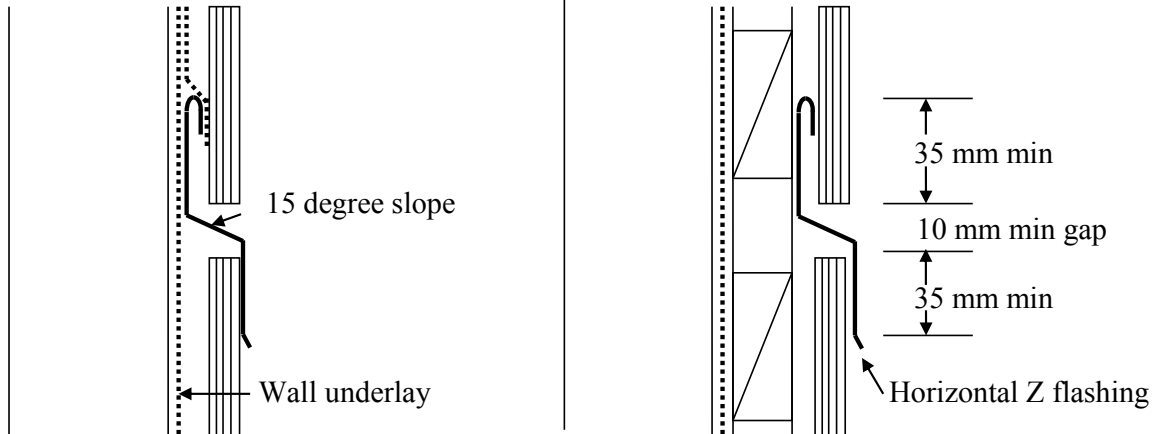
- an H jointer between direct-fixed fibre-cement wall panels
- a window head flashing in a cavity wall
- an apron flashing between a roof and a higher section of cavity wall.

Upstand heights in these joints have evolved from field experience. However, recent changes to extend the applicability of E2/AS1 (2011) to an extra high wind zone were responsible for precautionary increases to upstand heights in walls with cavities and direct-fixed claddings. These increases were from 35 to 60 mm for window head flashings and from 75 to 90 mm for roof to wall apron flashings. Another recent change required mandatory hems to the top of flashing upstands used in extra high wind zones. In lesser wind zones, the hem can be traded for an additional 25 mm of upstand height. These were largely precautionary changes ahead of applicable field experience or laboratory results of the type that this study aims to provide. Another significant change that came with wider adoption of cavity construction was the provision for vents in a cavity closer. Vents are air leakage paths and an entry point for air-carried spray. Once again, this project is setting out to link cladding overhang and clearances in joints with the effectiveness with which the joint rainscreens against water entry.

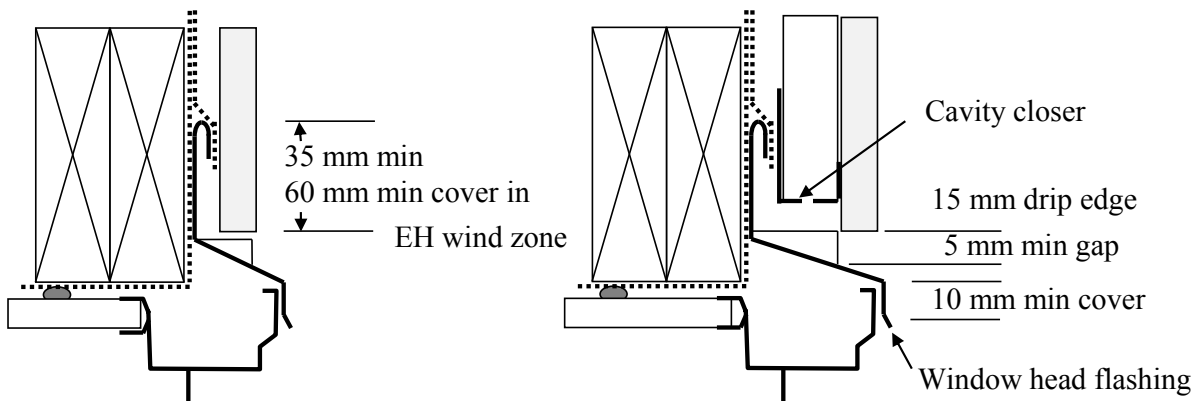
**Cladding is direct fixed**

**Cladding is on a cavity**

**Horizontal joint in plywood cladding**



**Window head with fibre-cement cladding**



**Apron flashings to metal roof**

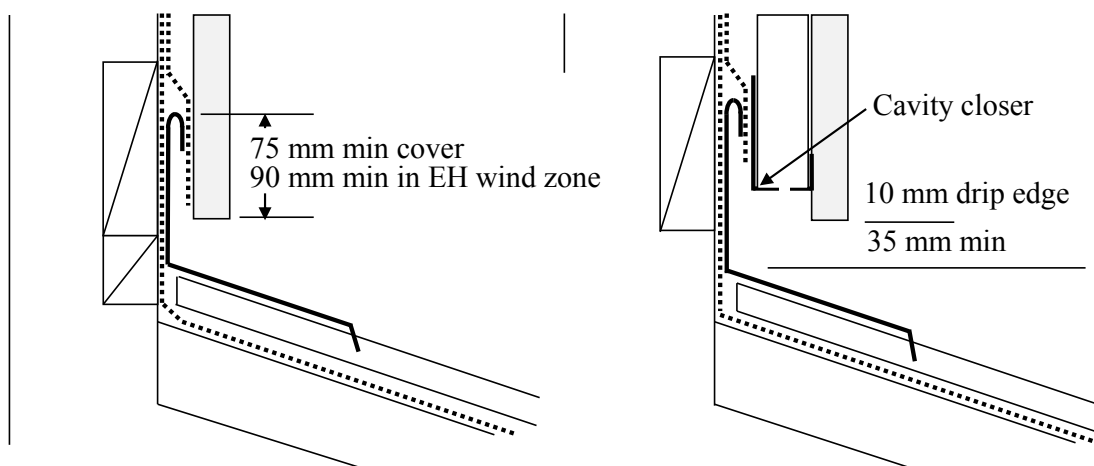


**Figure 4. A selection of flashings used in New Zealand buildings and taken from E2/AS1.**

## 5. LEAKAGE CHARACTERISTICS OF A HORIZONTAL CLADDING JOINTER

The leakage characteristics of a proprietary PVC H jointer were measured between two cladding panels fixed to cavity battens as illustrated in Figure 5. This is similar to the Z flashing illustrated in Figure 4 between plywood panels on a cavity wall except it does not include a hem now required in E2/AS1 in the extra high wind zone.

There are two main leakage paths of interest in the H jointer:

- Leakage between the upturned leg of the jointer and the cladding. Of particular significance are the offset space width ( $w$ ), the height of the upstand and the presence or absence of a hem folded into the upstanding leg.
- Leakage over the top of the lower cladding past the lower legs of the H jointer – not investigated here.

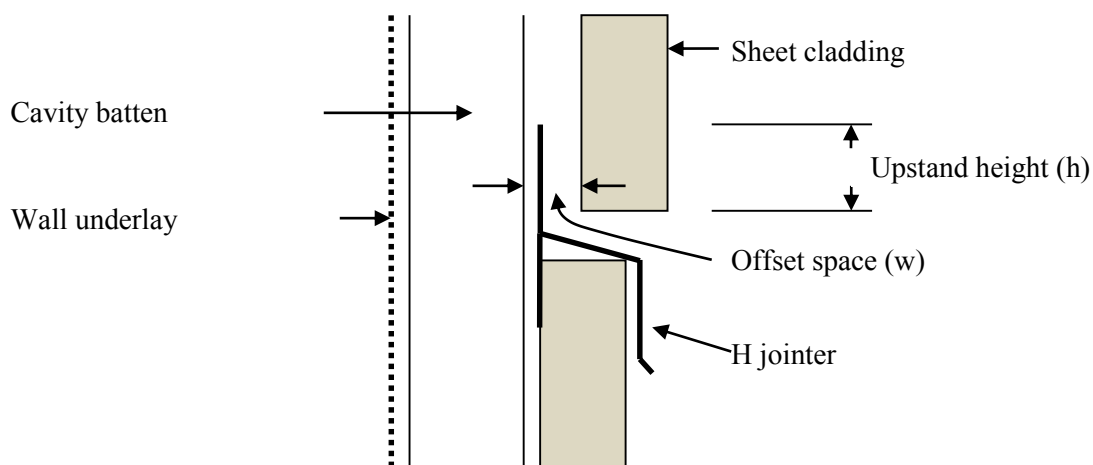


Figure 5. Sectional view through an H jointer between two sheets of wall cladding.

### 5.1 Significance of offset (air gaps) between the jointer and the cladding

The air pressure difference corresponding to the onset of leakage through the H jointer was measured with the equipment illustrated in Figure 2. A range of upstand heights were achieved by cutting down the upper leg of the jointer to 15 mm, 35 mm and 60 mm. A 530 mm wide section of jointer (spanning between cavity battens fixed to framing) was sprayed with water at 3.4 l/m<sup>2</sup>.min using the QPHA-2 nozzle. The air pressure difference was adjusted over the range 0–500 Pa until leakage was detected above the jointer. The pressure at which water breached the upstand is presented in Figure 6 for the three upstand heights, plotted against the offset width ( $w$ ). The pressures needed to spill water over the upstand were 147 Pa, 300 Pa and 588 Pa, corresponding to height ( $h$ ) values 15 mm, 35 mm and 60 mm. Water was seen at the top of the jointer at slightly lower pressures than these values (140 Pa, 294 Pa and 500 Pa with an uncertainty of 10 Pa). This will have been assisted by surface tension.

An effective capillary pressure can be calculated using the simplified Washburn equation (Straube and Burnett 2005) as follows:

$$P = \frac{2\sigma \cos\theta}{r}$$

where:

- $\sigma$  = the surface tension for water = 0.072 (N/m) at 20°C
- $\theta$  = the contact angle of water with the building materials (degrees)
- $r$  = the effective hydraulic radius for the opening (m)
- $w$  = the width of a crack between two sheet materials (m)
- $P$  = the capillary pressure (Pa)
- $h$  = the height of water supported in the joint between two sheets of building material (m)

The height of water supported in the joints studied here can be written as:

$$h = \frac{2\sigma \cos\theta}{g \rho w}$$

The contact angles appropriate to the two building materials in the joint (PVC and an acrylic painted fibre-cement board) have not been measured but have been taken as 85 degrees. This leads to a capillary pressure of 10 Pa with  $w = 1$  mm. While this will contribute to water being retained in the joint when the wind pressure relaxes, it will be necessary to reach the full static pressure equivalent of the joint to breach the upstand. When the offset gap  $w$  was increased, air-carried water leakage was observed as bubbling above the upstand. Figure 6 shows air-carried water leaks occurring at lower pressures as the offset gap is increased for all three upstand heights.

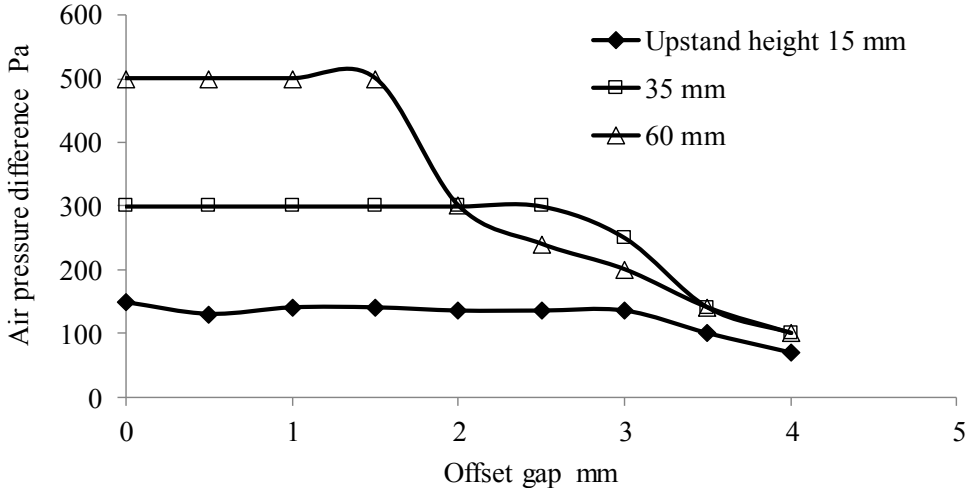


**Figure 6. Air pressures at which water leakage occurs through the H jointer as a function of upstand height and the offset gap width.**

### 5.2 Significance of a hem on the upstand of the jointer

The PVC H jointer was replaced with folded aluminium flashings having upstand heights of 35 mm and 60 mm and with and without a hem formed as illustrated in Figure 4. In this case, water leakage rates were measured gravimetrically over a period of 1 minute by weighing an absorbent strip placed just above the flashing. In all cases, the cladding was held against the flashing upstand ( $w = 0$ ). However, the flashings with a hem will have formed a 3 mm gap between the lower leg of the flashing and the back of the cladding. The Promax QPHA-1 Brown spray nozzle was fixed 1200 mm from the wall specimen to deliver 1.3 g/m.s of run-off over the joint. Static pressure leakage characteristics for the 35 mm and 60 mm high flashings are shown in Figure 7. These are similar to those measured earlier for the PVC H jointer, with the onset of leakage at 300 Pa and 500 Pa respectively. The onset of leakage was found to be independent of the hem. However, repeated measurements showed it was possible to achieve onset leakage pressures as high as 370 Pa and 580 Pa. This was done by carefully spring loading the hem of the 35 mm and 60 mm high flashings against the cladding. Although these measurements were conducted using standard construction materials, it is likely that the tolerances achieved in the laboratory were tighter than would be seen in buildings. Onset leakage pressures in the 100–300 Pa range indicated in Figure 6 for offset gap widths above 2 mm are more likely where no special care is taken to hold the flashing against the cladding. Higher upstand dimensions do bring weathertight performance advantages but only where air-carried water leakage can be eliminated with a tighter fit between flashing and cladding. Onset leakage pressures of 100–300 Pa are higher than the 50 Pa wetwall test pressure applied in E2/VM1 to the field of the cladding. On this basis, there is little argument for increasing upstand heights.

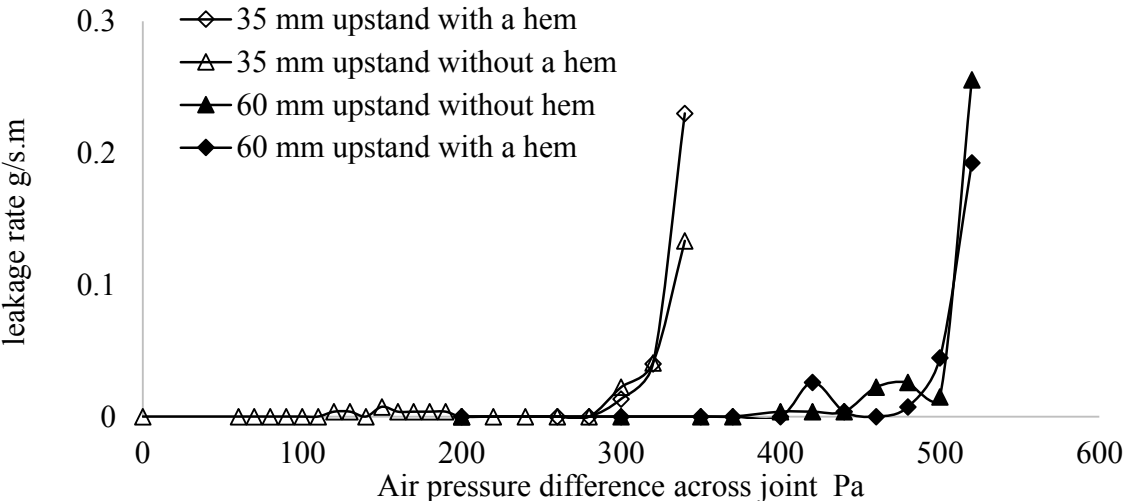
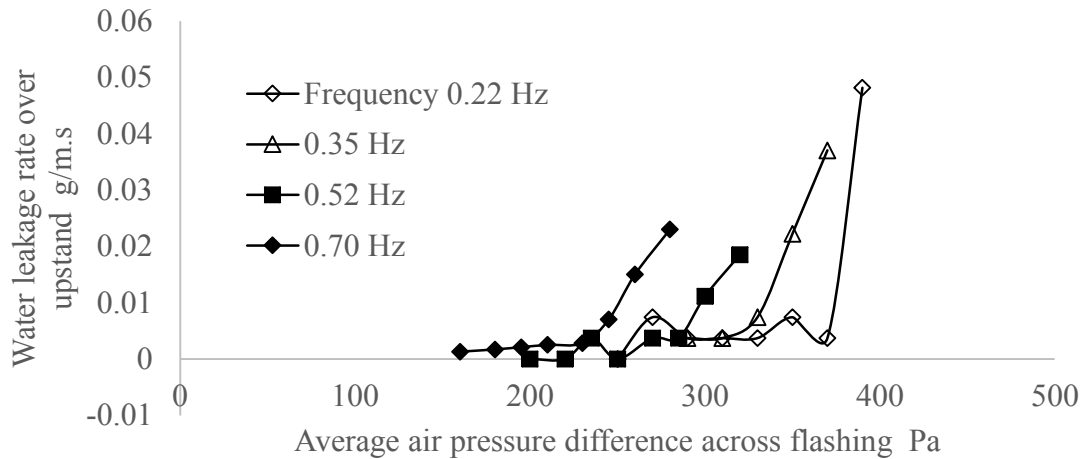


Figure 7. Steady pressure leakage characteristics of flashings with 35 mm and 60 mm upstands with and without hems.

Results of a more detailed study of the 35 mm high flashings applying static and fluctuating pressures are presented in Figure 8. Here, the water leakage rate is plotted against the peak air pressure difference and appears to indicate leakage rates at lower pressures as the frequency of the applied pressure increases. In fact, there was insufficient adjustment in the stroke of the fluctuating piston to keep the amplitude of the applied pressure independent of frequency, so the following additional analysis has been required.



**Figure 8. Dynamic leakage characteristics of flashings with a 35 mm upstand and a hem.**

Observations showed that water accumulating inside and relaxing out of the joint was in phase with pressure fluctuations up to 0.7 Hz. This suggests that the leakage rate at any time in the cycle might simply be calculated from the steady pressure leakage rate function and the applied sinusoidal pressure as follows:

The applied pressure difference  $\Delta p = A + B \sin \omega t$

where:

$\Delta p$  = the applied pressure difference (Pa)

$A$  = the average pressure (Pa)

$B$  = the amplitude of pressure fluctuation (Pa)

$\omega$  = the frequency of the fluctuating pressure (rad/s)

$L$  = the instantaneous joint leakage rate (g/m.s) and average leakage rate ( $L_{av}$  g/m.s)

where the static leakage function is a function of the pressure  $L = f(\Delta p)$

and the average leakage rate  $L_{av} = \frac{\omega}{2\pi} \int_0^{2\pi/\omega} f(A + B \sin \omega t) dt$

Calculated and measured leakage rates are plotted in Figure 9 for the 35 mm flashing with a hem. For these measurements, the hem was spring loaded against the back of the cladding to improve measurement repeatability, and average leakage rates were calculated numerically using the appropriate steady pressure leakage function.

The slope of the fitted line in Figure 9 is 1.06 with  $r^2 = 0.75$ . This indicates that leakage rates calculated on the basis of there being no significant inertia in the physical system agree reasonably well with measured data up to a frequency of 0.7 Hz. Higher frequencies than this are less important. A model that factors in the supply rate of water to the joint, inertia of water filling the joint and relaxation time for water draining from the joint has not been pursued.

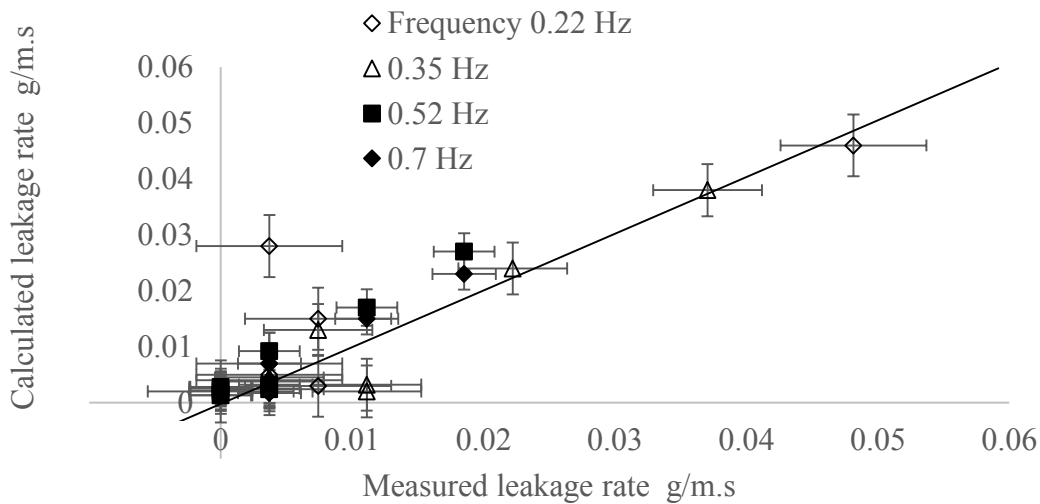


**Figure 9. A comparison of measured and calculated leakage rates with fluctuating air pressures.**

A similar dynamic pressure response was seen with the same height flashing (35 mm) without a hem. In this case, leakage rates were higher because it was less easy to clamp the flashing against the cladding over its entire length. Once again, there was no evidence for frequency-dependent leakage characteristics below 0.7 Hz.

## 6. LEAKAGE CHARACTERISTICS OF CAVITY CLOSER IN A WINDOW HEAD JOINT

A window head joint was assembled as in Figure 10 but with the capacity to adjust the position of the upper cladding in relation to the window head flashing. This allowed for some variations in joint dimensions, in particular, the gap between cladding and flashing (g).

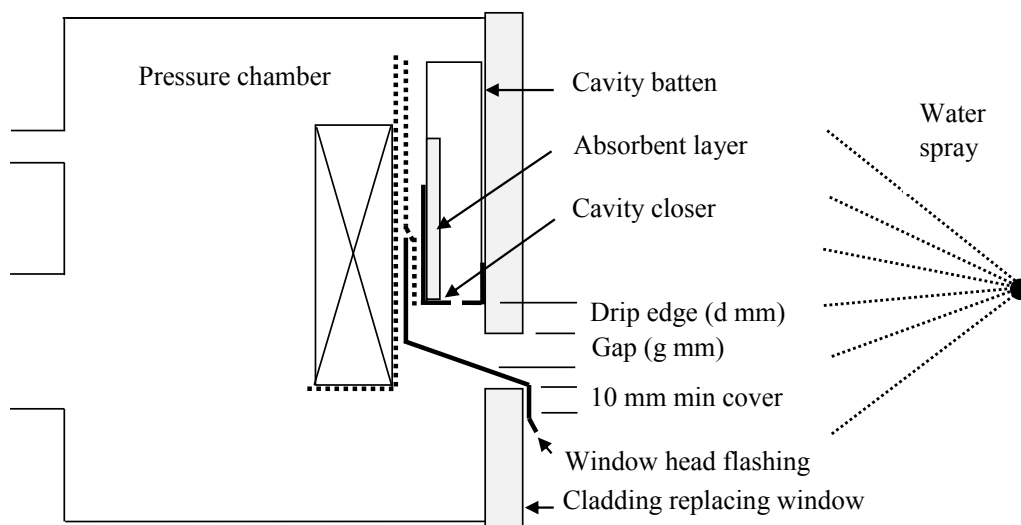


**Figure 10. Experimental window head joint with cavity closer and variable joint dimensions.**



There are four potential water leakage paths above the window flashing in Figure 10:

- Between the head flashing upstand and the cavity closer, which is essentially the leakage path examined earlier.
- Up through vent openings in the cavity closer as examined here.
- Past the stop-ends on the head flashing – not dealt with here.
- Under the flashing over the lower cladding – not dealt with here.

The upstand height of the head flashing above the base of the cavity closer is shown in Figure 4 to be 20 mm (45 mm in an extra high wind zone). In practice, the upstand on commercially available cavity closers is around 75 mm, significantly increasing the upstand against water leaking through vent openings in the cavity closer. The vent area at the base of the cavity closer was 1500 mm<sup>2</sup>/m made up of a series of slots 3 mm wide by 13 mm long. This exceeds the minimum vent area of 1000 mm<sup>2</sup>/m required by E2/AS1 (2011) at the base of a wall cavity. Water leakage rates through the cavity closer were measured as a function of the steady air pressure across the joint and plotted against the distance travelled up the upstand. This was achieved by segmenting the absorbent layer into nine parallel strips that could be individually weighed and assigned to a height above the cavity closer. The water spray rate was adjusted to 3 l/minute.m<sup>2</sup> using the Promax QPHA-2 Gray nozzle positioned 620 mm from the flashing. This aligns with the irrigation rates required in E2/VM1 (2011), and Figure 11 shows the deposition rates plotted against height above the cavity closer.

It is clear that higher pressures than the 50 Pa wetwall test pressure were required for detectable water to enter the cavity closer and reach the dry side of the cavity. However, the leakage onset pressures are considerably lower than for the H jointers discussed earlier. In fact, the onset leakage pressures for leakage above 35 mm and 60 mm are in the range 100–125 Pa compared with 300 Pa and 500 Pa for the H jointer. This indicates that the airtightness of the joint and other aspects of joint configuration are important. These pressures are still well ahead of the wetwall test pressure of 50 Pa in E2/VM1 (2011) for water reaching the back of the cavity. They are therefore ahead of the minimum weathertight performance expected of a residential cladding.

In practice, a significant proportion of wind pressure on a wall will lie across other components such as the internal lining and underlay. This is especially above a window, which effectively partitions the wall cavity for pressure moderation across wet joints in the cladding. Secondly, it is important to acknowledge the value of ventilation drying in both cavity walls and with direct-fixed weatherboard claddings. While the vents associated with window head flashings might reduce onset pressures for water leakage, the pressures are still well ahead of the wetwall test pressure of 50 Pa in E2/VM1 (2011). The potential for ventilation drying in cavity walls and behind direct-fixed weatherboard walls is shown in WALLDRY-NZ (Bassett et al. 2012). This provides the secondary water management needed to cope with even quite leaky claddings and to offset some loss in onset leakage pressures across window head flashings.

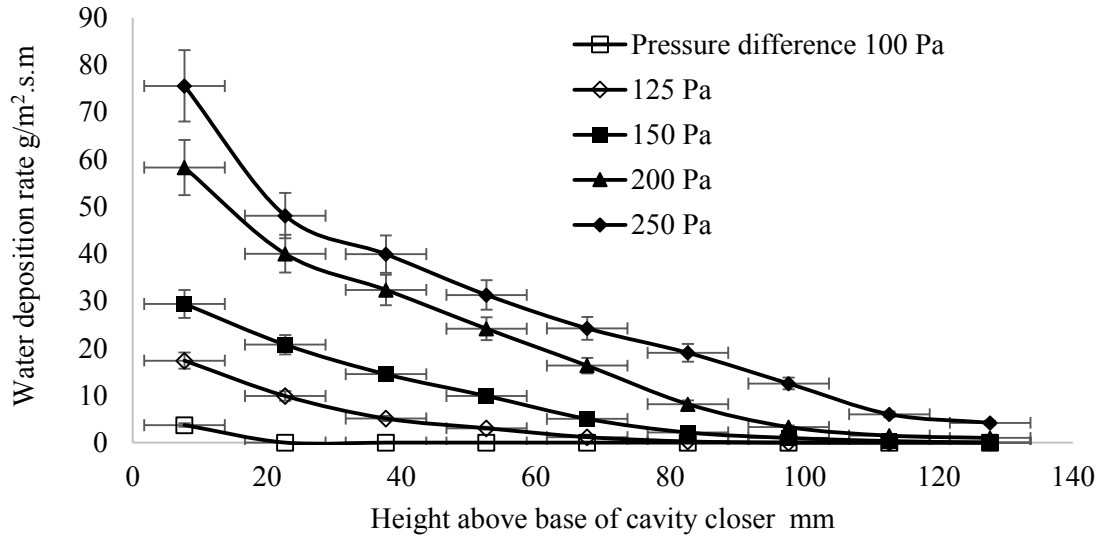


**Figure 11. Deposition rate of water as a function of height above the cavity closer.**

It was observed that water leakage past the cavity closer depended on a sufficiently high run-off rate past the window head, which effectively filled the joint and restricted the air flow into the cavity. This suggests that the water leakage rate may depend on dimensional factors that could be optimised to improve the water leakage characteristics of this head joint. The following factors have been investigated in sequence:

- Dependency on run-off rate over the joint achieved with a range of water spray nozzles.
- The gap between cladding and flashing (g).
- Whether the pressure was applied statically or dynamically.

## **6.1 Dependency of onset leakage pressures on run-off rate**

The net water leakage rate into the cavity closer was measured at run-off rates of 0.6–12 g/m.s over the window head joint. (This is equivalent to surface flow rates of 0.08–1.7 l/m<sup>2</sup>.min on the limited wall area above the head joint.) Figure 12 plots the steady pressure difference at which water first penetrated the cavity closer against the run-off rate over the window head joint. During these measurements, the joint dimensions were fixed at those shown in Figure 10 with a 5 mm gap between cladding and the head flashing. Two water leakage regimes were observed, as illustrated in Figure 12. Above a run-off rate of 2 g/m.s, water tended to bridge across the joint. This partially filled the space below the cavity closer and allowed water to be carried past the cavity closer at relatively low pressure differences. At run-off rates below 2 g/m.s, the joint drained out, with the smaller water leakage at higher pressures being attributed to air-carried spray.

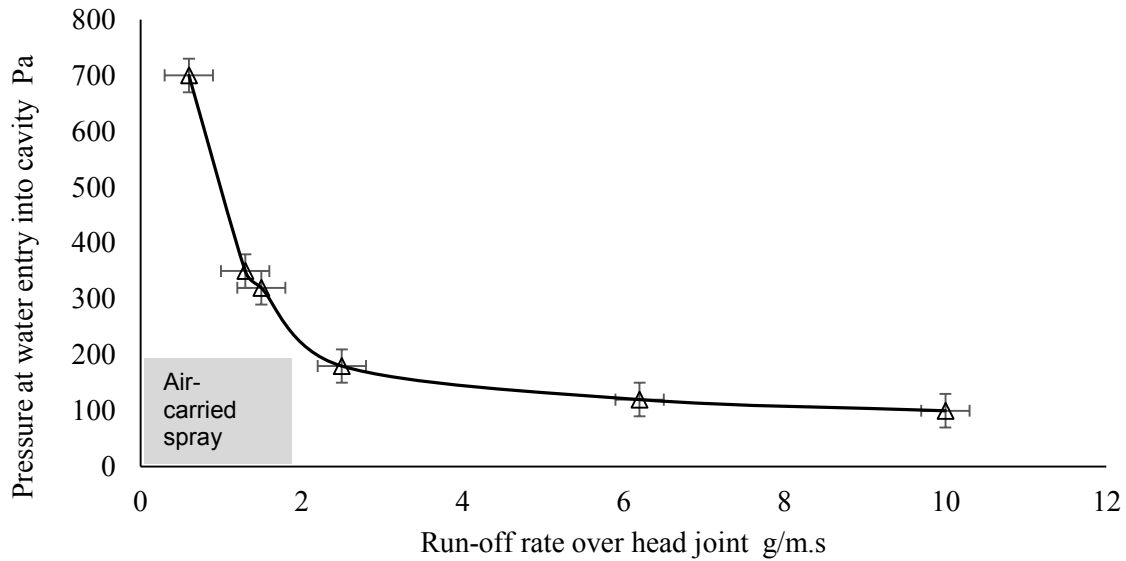


**Figure 12. Pressure difference at the onset of leakage through a window head joint as a function of run-off rate over the joint.**

## 6.2 Dependency of onset leakage pressures on gap between cladding and head flashing

These observations suggested that the cladding to head flashing dimension might be an important factor in the weathertight performance of this joint. A separate sequence of leakage measurements was carried out to investigate this possibility, with the gap width ( $g$ ) ranging from 1 mm to 9.6 mm. In Figure 13, the joint drained out more effectively with larger gap ( $g$ ) dimensions, and this could be worth exploring more in the context of taller buildings exposed to higher wind pressures. Below a gap width of 5 mm, the leakage performance of the joint appears to improve marginally. However, it has to be remembered that this is at the expense of free drainage from the joint.

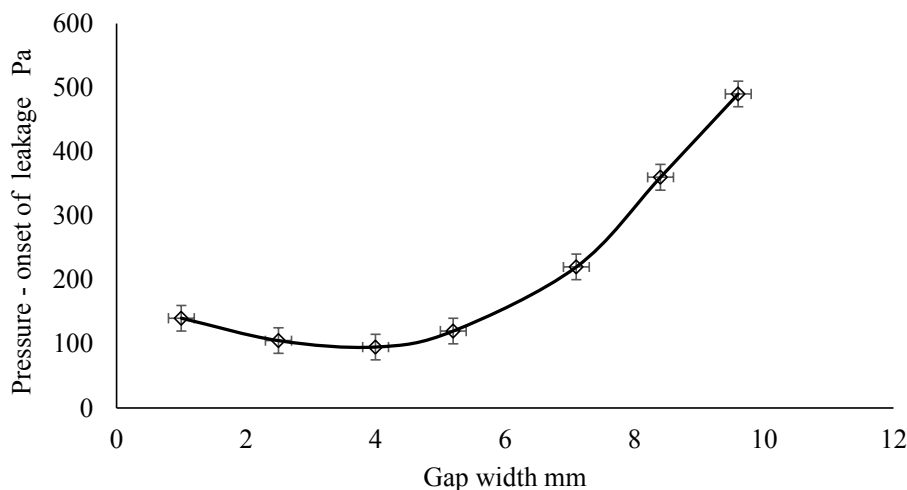


**Figure 13. Dependence of onset leakage pressure on gap width for the window head joint and the run-off rate set at 2 g/m.s.**

Figure 14 provides a pictorial view of leakage through a window head joint with varying surface run-off rates and gap dimensions between upper cladding and head flashing. It shows that increasing the cladding to sill tray gap ( $g$ ) improved the capacity of the joint to deal with high

run-off rates. However, this might also be achieved in other ways, for example, by adding a small kick-out to the lower edge of the cladding to deflect water from the opening.

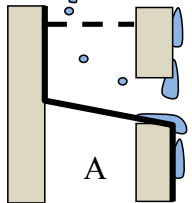
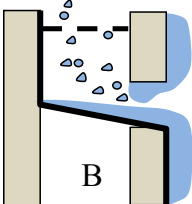
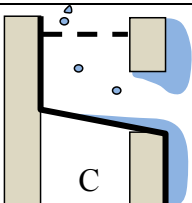
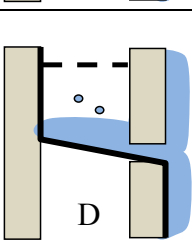
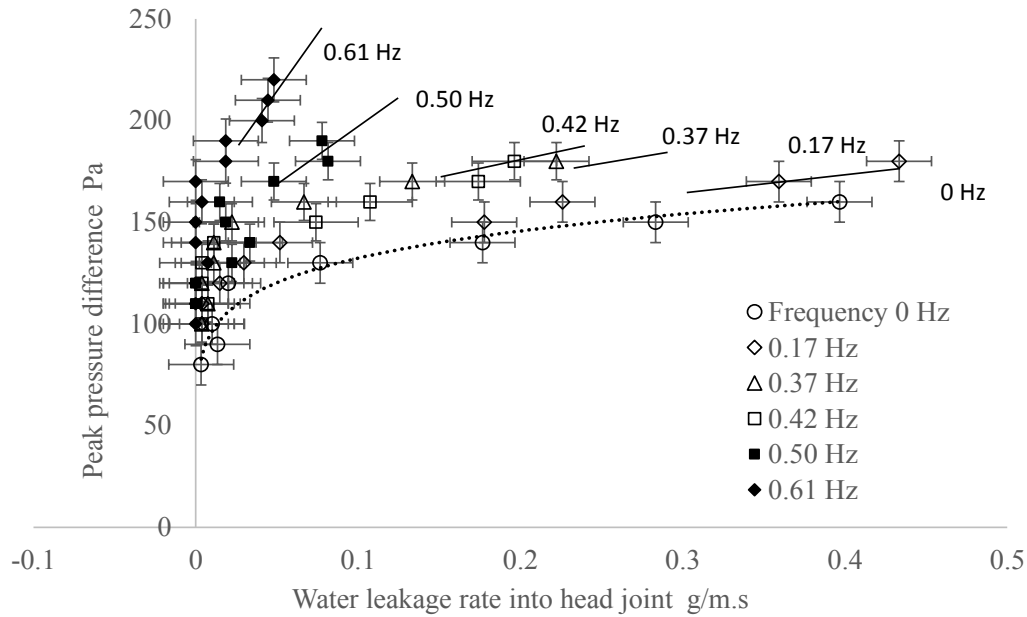
	<p><b>Case A:</b> Gap width (<math>g</math>) = 5 mm and the run-off rate is less than 2 g/m.s. The gap is not significantly occluded by run-off, and the flashing drains out effectively. Above a wind pressure of 200–300 Pa, air flow through the joint entrains small droplets, which pass through into the cavity.</p>
	<p><b>Case B:</b> Gap width (<math>g</math>) = 5 mm and the run-off rate is larger than 2 g/m.s. The gap is now occluded by run-off, and sufficient wind pressure is supported at the outer joint to drag water into the joint. Higher air velocities through the occluded opening drag water past the cavity closer at pressure differences around 100 Pa.</p>
	<p><b>Case C:</b> Gap width increased to (<math>g</math>) = 8 mm and the run-off rate is the same as Case A (below 2 g/m.s). The gap is no longer occluded by run-off, and the flashing drains out effectively. Beyond a wind pressure of 350 Pa, air flow through the joint entrains small droplets with leakage rates (0.015 g/m.s at 360 Pa).</p>
	<p><b>Case D:</b> Gap width decreased to (<math>g</math>) = 3 mm and the run-off rate is unchanged at 2 g/m.s. Now the gap is almost entirely occluded by run-off, and the flashing does not drain until both the wind pressure and run-off rate relax. Water leakage past the cavity closer is initially low but increases rapidly when the pressure difference exceeds the hydrostatic head distance (<math>d</math>) to the cavity closer.</p>

Figure 14. A pictorial view of leakage through a window head joint with varying surface run-off rates and gap dimension ( $g$ ) between upper cladding and head flashing.

### 6.3 Leakage with dynamic wind pressures applied

Water leakage of the window head joint was measured with dynamically applied air pressures in the 0–0.6 Hz range. During these measurements, the geometry of the joint was as shown in Figure 10, and the run-off rate over the joint was constant at 2.5 g/m.s. The pressure amplitude was adjusted to fall to a zero minimum where possible, but at low frequencies, there was not enough travel in the oscillating piston to achieve the full pressure amplitude. The water leakage rates into the cavity closer have been plotted in Figure 15 against peak air pressure for five frequencies in the range 0–0.61 Hz. There is a clear trend for the leakage characteristic to converge on the static pressure result at low frequencies, but it diverges towards much lower leakage rates at higher frequencies. This is a different result to that for H jointers between direct-fixed wall panels. Here, the leakage rate appeared to be in phase with varying wind pressures and was insensitive to frequency sensitivity in the range 0–0.7 Hz.



**Figure 15. Frequency dependency of relationship between peak pressure and water leakage into a window head joint.**

A two-phase flow analysis of the water leakage process in construction joints is outside the scope of this study. However, the question of whether the leakage rates shown in Figure 15 can be derived from the instantaneous leakage rates as for H and Z jointers has been addressed in Figure 16. Here, the instantaneous leakage rates over a full cycle have been calculated from the steady pressure results as described earlier and the calculated values compared with measured leakage rates. It is clear that leakage rates for frequencies below 0.4 Hz can be calculated from the steady pressure leakage data. However, at higher frequencies, inertia and the time constant of the joint cavity filling and drainage processes will have to be accounted for. There is room for further development of the leakage rate dependency on fluctuating pressures.

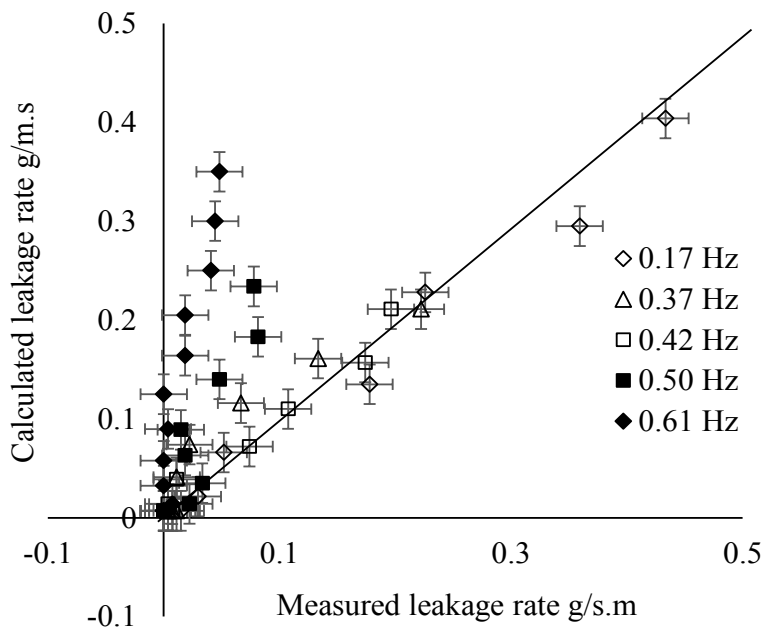


**Figure 16. A comparison of measured and calculated leakage rates using a simplified model.**

## 7. LEAKAGE CHARACTERISTICS OF AN APRON FLASHING TO ROOF JOINT

An apron flashing was assembled as shown in Figure 17 with the cavity wall details given in Figure 4. The apron flashing was simplified to a single piece of folded aluminium with an upstand height (distance from base of cladding to top of hemmed upstand) of 75 mm. The complete wall specimen measured 2.4 x 2.4 m, and a portion of the wall cladding was made removable to retrieve and weigh the absorbent layer. The leakage characteristics of the joint were measured statically as a function of run-off rate following the methods used for the window head flashing. Then the static spray bar was replaced with a 1 m diameter fan capable of driving water spray at the joint with air velocities up to 17 m/s. This allowed the leakage due to wind-carried rain to be compared from that due to run-off.

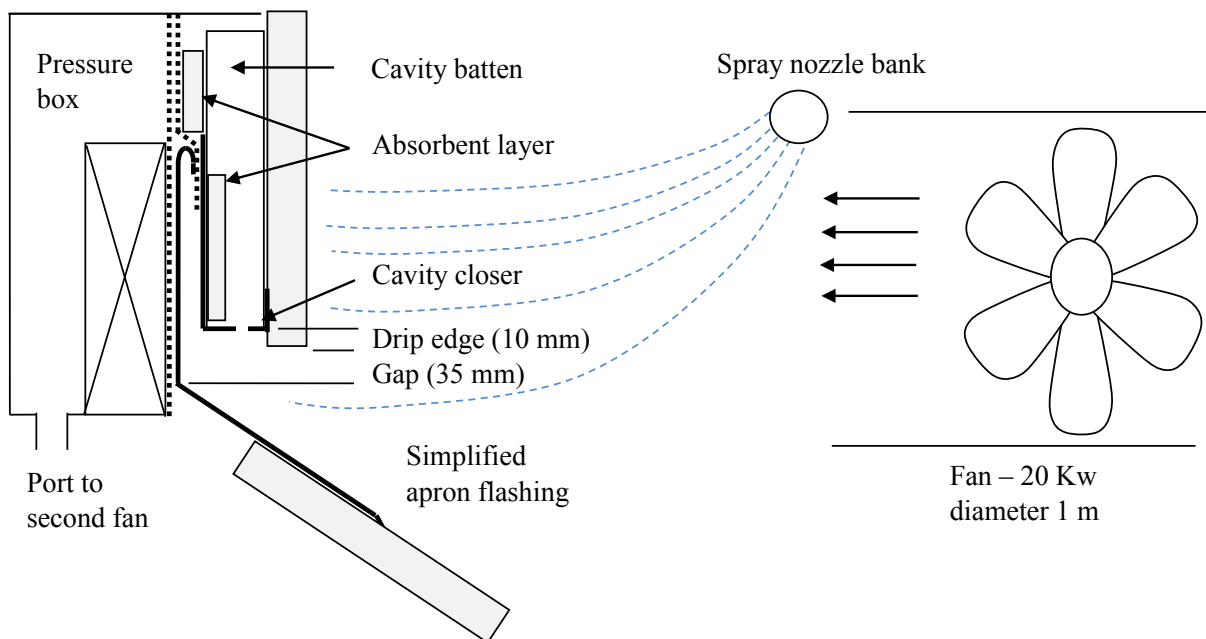


**Figure 17. Experimental apron flashing joint between roof.**

Four potentially significant water leakage paths past the apron flashing in Figure 17 are as follows:

- Between the flashing upstand and the cavity closer.
- Up through vent openings in the cavity closer.
- Past the ends of the apron flashing – not dealt with here.
- Under the flashing over the roof deck – not dealt with here

Leakage characteristics of a 1.2 m section of joint were measured with a 75 mm flashing upstand, a cavity closer upstand of 75 mm against the flashing and a smaller 18 mm upstand against the back of the cladding. The vent area in the cavity closer was 1500 mm<sup>2</sup>/m made up of a series of slots 3 mm wide by 13 mm long. It was the same cavity closer present in the window head joint studied earlier. Run-off rates over the joint in the range 3–60 g/m.s were achieved using water sprays shown in Table 2.

**Table 2. Spray nozzle operating conditions and run-off rates over the joint.**

Nozzle description	Number of nozzles	Water pressure (bar)	Stand-off (m)	Run-off rate (g/m.s)
Promax QPHA-1.5 White	2	2.8	1.2	3.8
Promax QPHA-2 Gray	2	2.8	1.2	13.5
Promax QPHA-5 Green	2	2.8	1.2	22.2
Promax QPHA-6.5 Yellow	3	2.8	1.2	54.2

Water leakage rates were measured inside the cavity closer against the taller leg at the back of the cavity and directly above the flashing. No water entry was detected above the 75 mm flashing upstand, due to the hem fitting tightly against the cavity closer and effectively closing off air leakage paths in this area. For this reason, the alternative flashing with a 90 mm upstand for extra high wind zones was not installed. As with the window head flashing, water entered through ventilation holes in the cavity closer, and leakage rates were measured at four run-off rates and air pressure differences in the range 0–1300 Pa. Leakage rates into the cavity closer are plotted in Figure 18, indicating no obvious relationship with either the pressure difference or the run-off rate. The joint behaved like a window head joint with a large gap between cladding and flashing that prevented the joint from filling up with water at even the highest run-off rates (see Figure 12). The measured leakage rates were small compared to those measured into the window cavity closer and were entirely due to small droplets of spray carried by air flows through ventilation holes in the cavity closer. Little information was available on the drop size distribution of the nozzles except the manufacturer’s claim of volume mean diameters in the range 0.85–2.8 mm for full cone nozzles of this type.

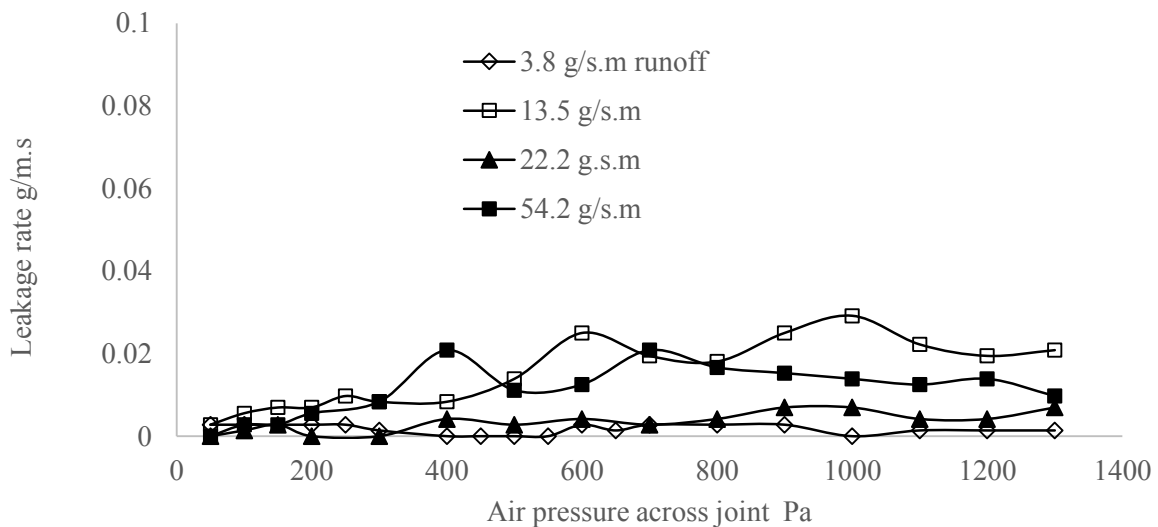


**Figure 18. Water leakage rates through the cavity closer above an apron flashing.**

## 7.1 Wind-driven water leakage past the apron flashing

The apron flashing specimen was positioned 6 m from the front of the large fan and the static air pressure measured at the joint. At maximum fan speed, this was 168 Pa – equivalent to an air speed of 16.7 m/s and well short of the pressures applied in E2/VM1 for buildings located in very high and extra high wind zones. The E2/VM1 test sequence does not simulate wind-carried driving rain and so the test parameters appropriate to buildings in New Zealand have yet to be developed. This means that the measurements described here are at best exploratory

of the leakage characteristics of a joint in buildings that has been known to take on water from wind-driven rain. The sprays positioned above the fan outlet delivered 16 l/min or an average of 2.8 l/m<sup>2</sup>.min over the specimen.

The rate of water entry into the cavity closer was measured as a function of the air pressure difference across the joint and the height of water penetration on the plane of the wall underlay. As in the earlier measurements, there was no leakage past the top of the 75 mm apron flashing but significant quantities of water entered through vents in the cavity closer. The air pressure difference across the cavity closer was adjusted from the baseline 168 Pa in steps of 200 Pa to 1168 Pa using the second fan indicated in Figure 17. Figure 19 shows the water entry rate plotted against height above the base of the cavity closer. This time, the water entry rate is plotted on a log scale to illustrate the large difference between water entering the joint and carried through the cavity closer to higher levels by air flows.

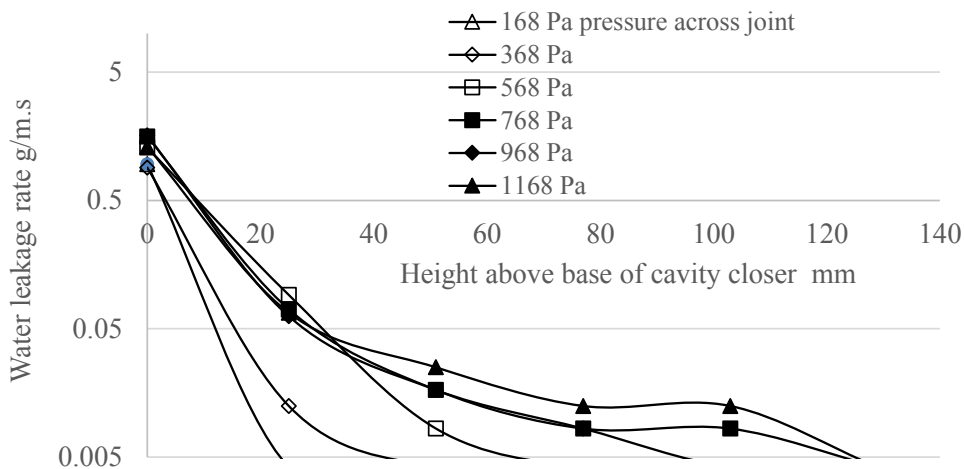


**Figure 19. Mass flow of water reaching various heights above the base of the cavity closer of an apron flashing.**

The leakage characteristics involve two processes. The first involves raindrops bouncing off the apron flashing and being carried by momentum into the base of the cavity closer. From here, they travelled no further unless significant air pressure differences greater than 100 Pa were present. The second process involved smaller droplets entrained in air flows reaching higher into the joint. The first process delivered large quantities of water, and the second delivered water flows that were similar to those measured earlier with static sprays. It is clear from Figure 19 that very large leakage rates are possible into the base of the cavity closer. However, at this stage, there have been no measurements of the frequency dependency of these water entry rates.

## 8. CONCLUSIONS

Preliminary weathertight performance measurements were carried out on three flashed joints in the NZBC compliance document E2/AS1 (2011). Water leakage rates were measured as a function of rain load, air pressure difference (statically and dynamically applied) and, in one case, with the rain load driven by high wind speeds and carrying momentum. In all of the joints studied, the water leakage performance limit was found to depend on the presence of air leakage paths. These were either in the form of vents in cavity closers or due to some misfit between flashings and claddings. For this reason, it is likely that field performance will be well



short of the leakage onset pressures measured here for ideal joints. Bearing in mind this limitation, the following conclusions were drawn:

- **H jointers between sheets of cladding.** Water leakage over the upstands of these flashings depended on the presence of gaps between flashing and cladding. With the flashing close fitting, the joint remained weathertight up to pressures close to the head of water equivalent of the upstand height. In more realistic building applications where the gap between flashing and cladding might exceed 2–3 mm, air-carried water leaks were seen at lower leakage onset pressures (100–300 Pa). There was little dependency on upstand height and the presence of a hem. Water leakage rates through tight-fitting joints were measured with dynamic pressure in the range of 0–0.7 Hz. There was no detectable effect of inertia, with measured water leakage rates agreeing with calculations using static pressure leakage characteristics.
- **Window head flashing in a cavity wall.** The onset of water leakage pressure through the vents in the cavity closer was 100 Pa. Past the 75 mm upstand leg of the cavity closer, it was much higher (150 Pa) when the flashing upstand fitted tightly against the cavity closer. These onset leakage pressures are much higher than the 50 Pa wetwall test pressure adopted in E2/VM1 for claddings but lower than the onset leakage pressures of ideally fitted H jointers between wall claddings. This difference is attributed to air leakage paths through vents in the cavity closer, which are necessary for drainage and ventilation drying in cavity walls. The leakage onset pressure for these joints in their standard form was found to depend on the run-off rate over the joint and on the gap between the cladding and head flashing. This could lead to opportunities to optimise joint designs for tall buildings. The dynamic leakage characteristics were quite different to those at static pressures, unlike the case for H jointers. Leakage rates at frequencies above 0.4 Hz were over predicted by the simple instantaneous pressure model. This will therefore require a model involving the inertia of water in the joint and the filling and drainage time constants.
- **Apron flashing between wall and roof.** The 35 mm gap between the base of the wall cladding and the apron flashing prevented high run-off rates from accumulating water in the space below the cavity closer. As a consequence, only very small air-carried water leaks through the cavity closer were detected up to very high air pressure differences when water was provided by static water sprays. Leakage rates a hundred times this were measured with rain driven at the joint by 17 m/s wind speeds. The new water entry process involved large droplets bounced off the apron and entering the base of the cavity closer where water could be carried deeper into the joint by wind pressures. The 75 mm of upstand against the wall underlay was easily sufficient to prevent water reaching the wall underlay. No leakage was detected between the apron flashing upstand (75 mm above the base of the cladding) because the hem fitted tightly against the cavity closer upstand, eliminating air leakage paths.

All of the joints examined here were adequately rainscreened against gravity-driven water entry. In all cases, it was necessary to apply wind-driven rain or an air pressure difference to drive water through the joint. This study has identified several opportunities to improve the leakage characteristics of joints to handle run-off and higher wind pressures appropriate to tall buildings outside the scope of E2/AS1. The work is seen as the start of more comprehensive investigation.

## 9. ACKNOWLEDGEMENTS

This work was funded by the Ministry of Business, Innovation and Employment and the Building Research Levy. The assistance of Roger Stanford is gratefully acknowledged.

## 10. REFERENCES

- Bassett, M., Clark, S. and Camilleri, M. (2003). *Building weathertightness failures – associated risk factors*. Presented at the BETEC symposium on building science applications at Syracuse University, New York.
- Bassett M., McNeil, S. and Overton, G. (2012). *WALLDRY-NZ: An educational tool for rain loads and ventilation drying in cavity walls*. Proceedings of the 5<sup>th</sup> International Building Physics Conference, Kyoto, Japan.
- Bassett, M.R., Overton, G.E. and McNeil, S. (2014). *Water leakage through weatherboards and ventilation drying modelled in WALLDRY-NZ*. Proceedings of the ICBEST Conference Building for a Changing World, Aachen, Germany.
- Department of Building and Housing. (2011a). Approved Document E2/AS1 *External moisture*. Wellington, New Zealand.
- Department of Building and Housing. (2011b). Approved Document E2/VM1 *External moisture*. Wellington, New Zealand.
- Hazleden, D.G. and Morris, P.I. (1999). *Designing for durable wood construction: The 4Ds. Durability of Building Components 8*. Research Press, Ottawa.
- Ishikawa, H. (1974). *An experiment on mechanism of rain penetration through horizontal joints in walls*. Proceedings of the 2nd International CIB/Rilem Symposium on Moisture Problems in Buildings. Paper 2.3.1. Rotterdam, The Netherlands, 10–12 September.
- Lacasse, M.A., O'Connor, T.J., Nunes, S. and Beaulieu, P. (2003). *Report from Task 6 of MEWS Project – Experimental assessment of water penetration and entry into wood-framed wall specimens*. Research Report IRC-RR-133. Institute for Research in Construction, National Research Council of Canada, Ottawa, Canada.
- Morrison Hershfield Limited. (1996). *Survey of building envelope failures in the coastal climate of British Columbia*. Report for Canada Housing and Mortgage Corporation, Morrison Hershfield Ltd, Ottawa, Canada.
- Overton, G. (2013). *An analysis of wind driven rain in New Zealand*. Building Research Association of New Zealand. Study Report SR300.
- Sahal, N. and Lacasse, M.A. (2004). Water entry function of a hardboard siding-clad wood and stud wall. *Building and Environment*, 40, 1479–1491.
- Standards New Zealand. (2008). NZS 4211 *Specification for performance of windows*. Standards New Zealand, Wellington.
- Standards New Zealand. (2008). AS/NZS 4284 *Testing of building facades*. Standards New Zealand, Wellington.
- Standards New Zealand. (2002). AS/NZS 1170 *Structural design actions*. Standards New Zealand, Wellington.
- Straube, J. and Burnett, E. (2005). *Building science for building enclosures*. Building Science Press. Westford MA.
- Teasdale-St-Hilaire, A. and Derome, D. (2006). Methodology and application of simulated wind-driven rain infiltration in building envelope experimental testing. *ASHRAE Transactions*, 112(2), 656–670.